Accepted Manuscript

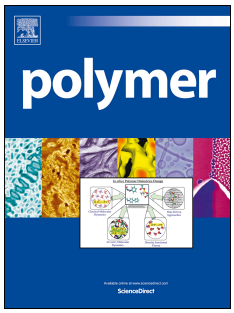

Analytical self-consistent field model of arm-grafted starlike polymers in nonlinear elasticity regime

E.B. Zhulina, V.M. Amoskov, A.A. Polotsky, T.M. Birshtein

PII: S0032-3861(14)00739-3

DOI: 10.1016/j.polymer.2014.08.047

Reference: JPOL 17215

To appear in: *Polymer*

Received Date: 10 July 2014

Revised Date: 18 August 2014

Accepted Date: 19 August 2014

Please cite this article as: Zhulina EB, Amoskov VM, Polotsky AA, Birshtein TM, Analytical self-consistent field model of arm-grafted starlike polymers in nonlinear elasticity regime, *Polymer* (2014), doi: 10.1016/j.polymer.2014.08.047.

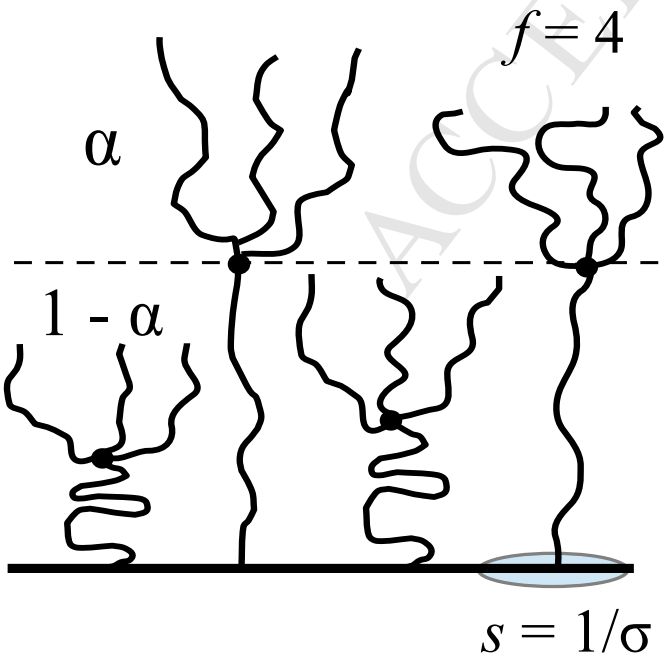

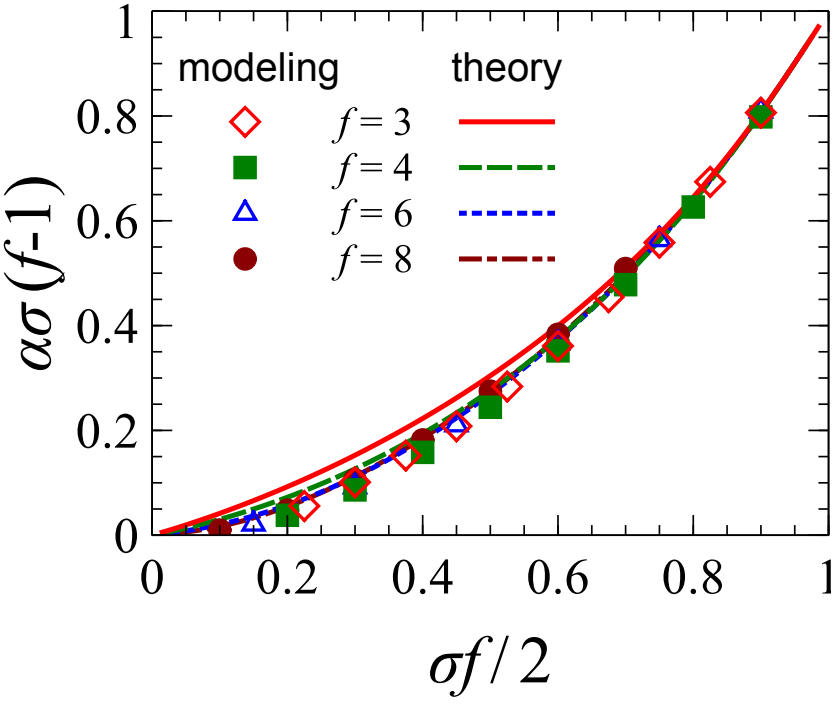

Analytical self-consistent field model of arm-grafted starlike polymers in nonlinear elasticity regime

E.B. Zhulina[1,2], V.M. Amoskov[1],
A.A.Polotsky*[,1,2], T.M.Birshtein[1,3]

[1]Institute of Macromolecular Compounds, Russian Academy of Sciences, 31 Bolshoy pr., 199004 Saint Petersburg, Russia
[2] Saint Petersburg National Research University of Information Technologies, Mechanics and Optics (ITMO University), Kronverkskiy pr. 49, 197101 Saint Petersburg, Russia
[3]Saint Petersburg State University, Department of Physics, 198504 Petrodvorets, Saint Petersburg, Russia

August 18, 2014

Abstract

We develop approximate analytical (AA) model to describe the structure of a brush made of starlike polymers (regularly branched dendrons of the first generation) grafted by one arm onto a planar surface. It is demonstrated that introduction of two sub-layers with distinct populations of strongly and weakly stretched dendrons allows for adequate semi-analytical description of these end-grafted macromolecules in nonlinear elasticity regime. We calculate brush thickness, fraction of strongly stretched dendrons and polymer density profiles as a function of polymer grafting density and number of branches in starlike macromolecule. The predictions of AA model are compared with the results of numerical self-consistent field model of Sheutjens and Fleer (SF-SCF). Good agreement between the two models is found at high grafting densities and/or at large number of branches of starlike polymers.

1 Introduction

Investigation of tethered layers of macromolecules (polymer brushes) has been intensified during the last decades initiated by the pioneering works of Alexander [1] and de Gennes [2]. The structure and properties of brushes formed by linear polymers are currently well comprehended, and there polymers are widely used in stabilization of colloidal systems [3], design of responsive, antifouling, and modulated surfaces, etc. [4, 5, 6, 7, 8]. End-grafted macromolecules with

*Corresponding author. E-mail: alexey.polotsky@gmail.com

more complex architecture (e.g., branched polymers) could mediate interactions between surfaces in architecture-dependent manner [10, 11] and lead to improved physical/chemical characteristics of modified substrates compared to linear grafted chains. However, the properties of end-grafted macromolecules with complex architecture are less understood that those of linear polymers.

Equilibrium properties of dendron brushes have been studied by means of the analytical and numerical self-consistent field theories, and computer simulations [12, 13, 14, 15, 16, 17, 18, 19, 20, 21, 22, 23]. The results of these studies were summarized in recent highlight article [24]. An elegant analytical description has been developed for a brush of regularly branched dendrons with linear (Gaussian) elasticity of the spacers [12]. The requirement of linear elasticity can be fulfilled at relatively sparse grafting of the dendrons with small number of generations. The equilibrium structure of a planar brush of dendrons of the first generation, that is, a brush of starlike polymers tethered to a planar surface by terminal segment of one of the star arms (referred to as *stem*) has been recently investigated in details by means of the analytical theory and the numerical Scheutjens-Fleer self-consistent field (SF-SCF) approach (SF-SCF) [17]. The analytical model took advantage of the parabolic molecular potential (which is applicable to tethered dendrons with the Gaussian elasticity [12]), whereas the numerical SF-SCF modeling accounted for the finite stretching of the tethered macromolecules. The analytical predictions and the numerical calculations demonstrated good agreement for the values of system parameters consistent with the Gaussian elasticity of the tethered dendrons. When however the stretching of tethered starlike polymers was approaching the linear elasticity threshold, the deviations between the analytical and the numerical results became significant. In particular, at high grafting density the numerical SCF model [15, 17, 24] indicated a segregation of starlike polymers in two distinct populations with weakly stretched and strongly (almost totally) stretched stems. The two-population structure of the star-brush was also confirmed by Langevin dynamics (LD) [16] and Brownian dynamics (BD) [18] simulations. The analytical model (implementing the Gaussian elasticity of dendrons) failed to do so.

The finite stretching of the densely tethered starlike dendrons has been recently taken into account by using a box-like model [19]. The latter incorporated two sub-layers with equal and uniform distribution of monomers. The first, (adjacent to the surface) sub-layer contained weakly stretched stars and strongly stretched stems of dendrons that delegate their branches in the second (upper) sub-layer. The upper sub-layer contained only branches of the strongly stretched dendrons and thereby constituted a brush of linear chains (branches). The tension in the strongly stretched dendrons was introduced by using the Padé-approximation for the inverse of the Langevin function [19] while excluded volume interactions were implemented through the Boublik-Mansoori-Carnahan-Starling-Leland (BMCSL) equation of state for hard-sphere systems [25]. The elastic contribution of weakly stretched dendrons in the first sub-layer was neglected. This model predicted the equilibrium fraction of strongly stretched dendrons as a function of the grafting density, and demonstrated a good correspondence with the results of supplementary LD simulations [16] performed for the starlike macromolecules.

The goal of this study is to develop an approximate analytical (AA) model that accounts for nonlinear extensibility of the starlike polymers and does not

assume *a priori* a uniform polymer density distribution in the dendron brush. A finite extensibility of tethered linear polymer chains was taken into account in the studies of Amoskov and Pryamitsyn [26, 27, 28]. They derived a self-consistent molecular potential (referred here as bcc-potential) that provides the force - distance relationship for a linear polymer on body centered cubic (bcc) lattice at any degree of the chain stretching. At low chain stretching the bcc-potential reduces to the parabolic off-lattice potential derived by Semenov [29] for tethered polymer chains with the Gaussian elasticity. In this study we combine the bcc molecular potential for linear chains, and the parabolic potential introduced by Pickett [12] for regularly branched dendrons. We analyze the equilibrium structure of a densely grafted planar brush of starlike polymers, and compare the predictions of the approximate analytical (AA) model with the results of SF-SCF calculations based on the Flory-Huggins theory of polymer solutions [17].

2 Model

The brush of dendrons of the first generation is formed by starlike macromolecules attached to a planar surface by the terminal monomer of one of the branches. Each starlike macromolecule has $f \geq 2$ identical branches with $n \gg 1$ monomer units of the size a. The overall number of monomer units is thus $N = nf$, the number of the free ends equals $f - 1$. The macromolecules are tethered to the surface with dimensionless grafting density σ (measured in units a^{-2}). In the dendron brush the equilibrium requires not only vanishing of the elastic tension at the free ends, but also the force balance at each branching point of a tethered dendron.

As long as the brush-forming chains are stretched with respect to the ideal chain dimensions and exhibit the Gaussian elasticity, the self-consistent molecular potential $U(z)$ acting on a chain segment at distance z from the grafting surface is given by

$$U(z) = \Lambda - \frac{3}{2}\left(\frac{Kz}{2na}\right)^2, \tag{1}$$

where Λ is a constant and the coefficient K depends on the total number of branches, f, as [17]

$$K = 2\arccos\sqrt{\frac{f-1}{f}}. \tag{2}$$

Here and below all energetic quantities are measured in units of k_BT.

The polymer density profile (volume fraction of monomer units) $\varphi(z)$ in such brush is specified by the density of the free energy of monomer-monomer interactions, $F_{int}\{\varphi(z)\}$, as [30]

$$U(z) \equiv \frac{a^3 \cdot \delta F_{int}\{\varphi(z)\}}{\delta\varphi(z)}. \tag{3}$$

Similarly to brush of linear chains, the dendron brush is characterized by (i) monotonous decrease in the stretching of spacers as a function of chemical distance from the focal point, and (ii) wide distribution of the end segments, that is, strong fluctuations in stretching of individual starlike macromolecules. This

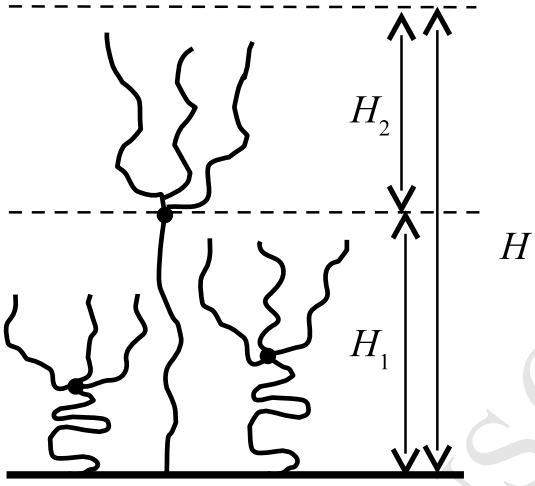

Figure 1: Schematic of starlike brush with two-layered structure adopted in the approximate analytical (AA) model.

distribution leads to smoothly decreasing polymer volume fraction profile $\varphi(z)$ which progressively flattens in the central region upon an increase in grafting density σ, and number of branches f .

Following the predictions of SF-SCF modelling [15, 17, 24], LD [16] and BD [18] simulations, and the box-like model of Merlitz *et al* [19], we divide the brush into two sub-layers (1 and 2) with thickness H_1 and H_2, respectively (see schematic in figure 1). The total brush thickness is $H = H_1 + H_2$. We assume that fraction α of stars have a strongly stretched stem and q free branches in the upper sub-layer (2). The branching points of these stars are fixed at distance H_1 from the grafting surface, i.e., at the boundary between the sub-layers 1 and 2. In the lower sub-layer 1 fraction $(1 - \alpha)$ of stars are weakly stretched, and these macromolecules exhibit the Gaussian elasticity on all length scales.

The bcc-potential for linear chains with length n is given by

$$U_{bcc}(z) = \Lambda + 3\ln\left(\cos\frac{\pi z}{2na}\right). \tag{4}$$

At small distances from the surface, $z/(na) \ll 1$, the potential in eq 4 reduces to the familiar parabolic potential [29]:

$$U_{bcc}(z) \approx \Lambda - \frac{3\pi^2}{8}\left(\frac{z}{na}\right)^2.$$

We *assume* that the molecular potential $U_1(z)$ acting on the monomers in the lower sub-layer 1 has the same functional form as the bcc-potential,

$$U_1(z) = \Lambda_1 + 3\ln\left(\cos\frac{Kz}{2na}\right) \tag{5}$$

but with the constant K specified for starlike polymers by eq 2. For weakly

stretched dendrons in the sub-layer 1 with the Gaussian elasticity (i.e., at distances $z/(na) \ll 1$), eq 5 reduces to the potential in eq 1.

The sub-layer 2 constitutes the brush of linear chains (branches) with length n and the grafting density $\sigma\alpha(f-1)$. The molecular potential for linear chains with length n is given by eq 4. Because the sub-layer 2 starts from $z = H_1$, the molecular potential $U_2(z)$ is simply the shifted bcc-potential,

$$U_2(z) = \Lambda_2 + 3\ln\left[\cos\frac{\pi(z-H_1)}{2na}\right] = -3\ln\left[\cos\frac{\pi(H-H_1)}{2na}\right] + 3\ln\left[\cos\frac{\pi(z-H_1)}{2na}\right],$$

with Λ_2 obtained from the condition $U_2(z=H) = 0$.

The required continuity of the molecular potential $U(z)$ at the boundary between sub-layers $z = H_1$ (i.e., $U_1(H_1) = U_2(H_1)$), allows to determine the constant Λ_1 in eq 5,

$$\Lambda_1 = -3\ln\left[\cos\frac{KH_1}{2na}\cdot\cos\frac{\pi(H-H_1)}{2na}\right].$$

The molecular potential $U(z)$ is then specified as

$$U(z) = \left\{\begin{array}{l} U_1(z) \\ U_2(z) \end{array}\right. = \left\{\begin{array}{ll} 3\ln\frac{\cos\frac{Kz}{2na}}{\cos\frac{KH_1}{2na}\cdot\cos\frac{\pi(H-H_1)}{2na})} & 0 \le z \le H_1 \\ 3\ln\frac{\cos\frac{\pi(z-H_1)}{2na}}{\cos\frac{\pi(H-H_1)}{2na}} & H_1 \le z \le H \end{array}\right. .$$

The Flory-Huggins polymer solutions theory specifies the density $F_{int}(\varphi)$ of the free energy of monomer-monomer interactions in solution (measured in units of k_BT per unit volume) with volume fraction φ of monomer units as

$$a^3 \cdot F_{int}(\varphi) = (1-\varphi)\ln(1-\varphi) + \chi\varphi(1-\varphi),$$

where χ is the Flory interaction parameter, and the translational contribution of polymer chains is omitted due to end-grafting of the starlike macromolecules. Under good solvent conditions at $\chi = 0$, the polymer density profile $\varphi(z)$ in the starlike brush is determined by equation 3 as

$$-\ln[1-\varphi(z)] = U(z)$$

and is given by

$$\varphi(z) = \left\{\begin{array}{l} \varphi_1(z) \\ \varphi_2(z) \end{array}\right. = \left\{\begin{array}{ll} 1 - \frac{(\cos\frac{\pi(H-H_1)}{2na})^3(\cos\frac{KH_1}{2na})^3}{(\cos\frac{Kz}{2na})^3} & 0 \le z \le H_1 \\ 1 - \frac{(\cos\frac{\pi(H-H_1)}{2na})^3}{(\cos\frac{\pi(z-H_1)}{2na})^3} & H_1 \le z \le H_1 + H_2 \end{array}\right. .$$

Normalization of the polymer density profile,

$$a^{-1}\int_0^{H_1}\varphi_1(z)dz = \alpha\sigma n + (1-\alpha)\sigma n f = \sigma n[f - \alpha(f-1)] \qquad (6)$$

and

$$a^{-1}\int_{H_1}^{H}\varphi_2(z)dz = \sigma n\cdot\alpha(f-1) \qquad (7)$$

provides two equations that link the three unknown variables: the thicknesses of sub-layers H_1 and H_2, and the fraction α of strongly stretched dendrons. The third equation is provided by the force balance at the boundary between two sub-layers.

2.1 Force balance

To formulate the force balance at the boundary between sub-layers we need to find the stretching function $E(z) = a^{-1} \cdot (dz/dn)$ of strongly stretched stems in sub-layer 1. This function is calculated in the Appendix A and is given by

$$E(z) = \sqrt{1 - \frac{1 - f\sin^2(KH_1/2an)}{\cos^2(Kz/2an)}} \tag{8}$$

Stretching $E(z)$ of the dendron stem at the boundary between sub-layers, $z = H_1$, yields

$$E(H_1) = \frac{\tan(KH_1/2an)}{\tan K/2}$$

and is related to a dimensionless tension force p acting in this stem at $z = H_1$ (see Appendix A) as

$$p(H_1) = \frac{3}{2}\ln\frac{1 + E(H_1)}{1 - E(H_1)} = \frac{3}{2}\ln\frac{\tan(KH_1/2an) + \tan(K/2)}{\tan(K/2) - \tan(KH_1/2an)}$$

Force per unit area $p(H_1)\alpha\sigma$ of the boundary between two sub-layers ($z = H_1$) must be balanced by the osmotic pressure $\Pi(H_1)$, measured in units of k_BT/a^3, which is related to the volume fraction $\varphi(H_1)$ as

$$\Pi(H_1) = -\ln[1 - \varphi(H_1)] - \varphi(H_1)$$

to ensure the force balance

$$p(H_1)\alpha\sigma = \Pi(H_1)$$

We now introduce the dimensionless variables,

$$h_1 = \frac{H_1}{2na}; \quad t = \frac{z}{2na}; \quad h_2 = \frac{H_2}{2na}$$

In these variables, the polymer density profile is presented as

$$\varphi(t) = \begin{cases} \varphi_{in}(t) \\ \varphi_{out}(t) \end{cases} = \begin{cases} 1 - \frac{(\cos\pi h_2)^3(\cos Kh_1)^3}{(\cos Kt)^3} & 0 \le t \le h_1 \\ 1 - \frac{(\cos\pi h_2)^3}{(\cos\pi(t-h_1))^3} & h_1 \le t \le h_1 + h_2 \end{cases}$$

and the force balance is formulated as

$$\frac{3}{2}\alpha\sigma\ln\frac{\tan(Kh_1) + \tan(K/2)}{\tan(K/2) - \tan(Kh_1)} = -3\ln\cos\pi h_2 - 1 + \cos^3\pi h_2 \tag{9}$$

After integration of the polymer density profiles in eqs 6 and 7 and introduction of reduced variables, eqs 6 and 7 reduce to

$$h_1 - \frac{\cos^3(\pi h_2)\cos^3(Kh_1)}{2K}\left[\frac{\sin(Kh_1)}{\cos^2(Kh_1)} + \ln\sqrt{\frac{1 + \sin(Kh_1)}{1 - \sin(Kh_1)}}\right] = \frac{\sigma f}{2} - \frac{\alpha\sigma(f-1)}{2} \tag{10}$$

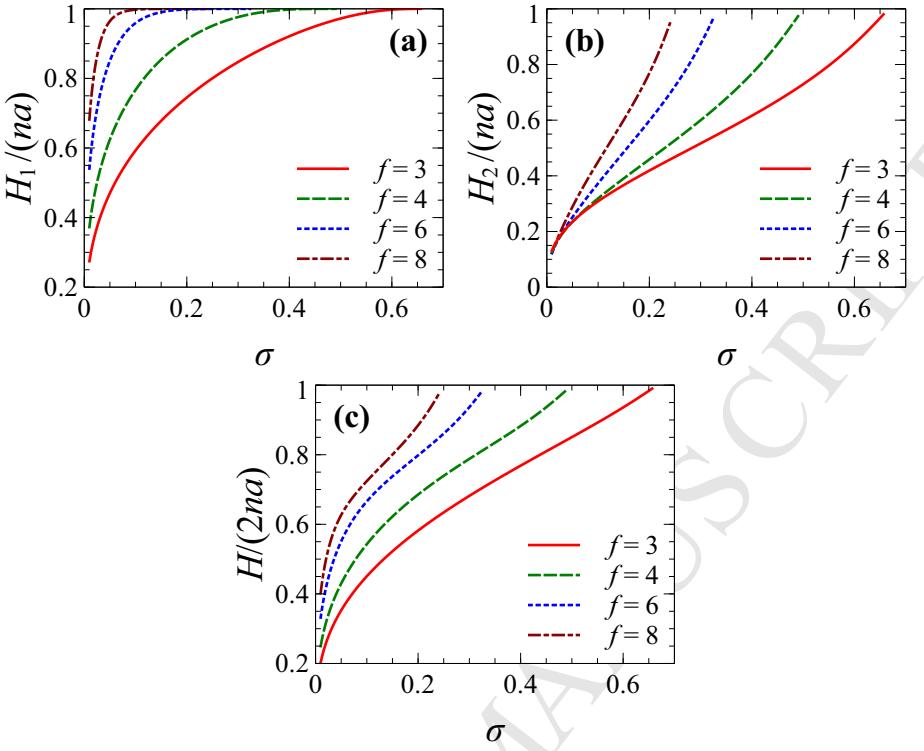

Figure 2: Reduced thickness $H_1/(na)$ of sub-layer 1 (a), $H_2/(na)$ of sub-layer 2 (b), and the total brush thickness $H/(2na)$ (c) as functions of dimensionless grafting density σ for different values of number of branches $f = 3$, 4, 6, 8.

and

$$h_2 - \frac{\cos^3(\pi h_2)}{2\pi}\left[\frac{\sin(\pi h_2)}{\cos^2(\pi h_2)} + \ln\sqrt{\frac{1+\sin(\pi h_2)}{1-\sin(\pi h_2)}}\right] = \frac{\alpha\sigma(f-1)}{2} \qquad (11)$$

The set of three equations (9, 10, and 11) allows us to find the three unknown variables: reduced thicknesses of sub-layers, $h_1$and h_2, and fraction α of strongly stretched dendrons at given values of constant K (eq 2), and grafting density σ of tethered starlike macromolecules. These equations are solved numerically (see Appendix B for details).

3 Results and discussion

Figures 2 demonstrate the thicknesses of sub-layers, $H_1/(an)$ (a) and $H_2/(an)$ (b), and the total brush thickness, $H/(2an)$ (c), predicted by the AA model as a function of dimensionless grafting density σ at various numbers of branches f.

As follows from figures 2a and 2b, dimensions of the first and second sub-layers, though both being monotonously increasing functions of σ, behave quite differently, especially for stars with large number of arms. The thickness of

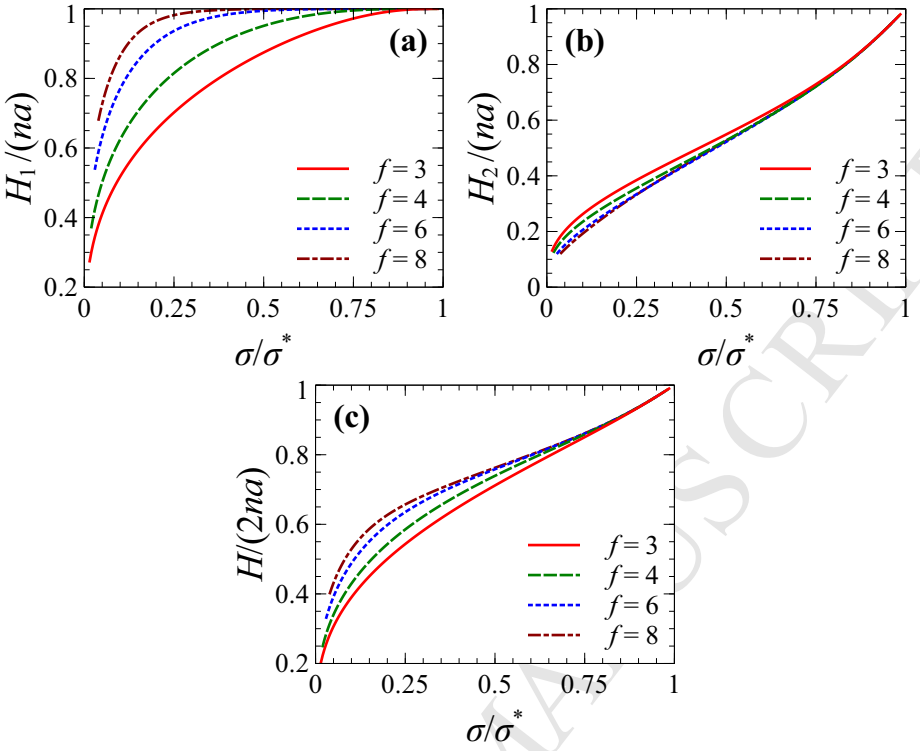

Figure 3: Reduced thickness $H_1/(na)$ of sub-layer 1(a), $H_2/(na)$ of sub-layer 2(b), and the total brush thickness $H/(2na)$ (c) as functions of normalized grafting density σ/σ^* for different values of number of branches $f = 3$, 4, 6, 8.

the first sub-layer H_1 increases sharply at small σ but approaches its limit at dense grafting smoothly. On the contrary, the steepness of the outer sub-layer thickness H_2 dependence on σ increases with increasing grafting density

Such qualitatively different behavior is attributed to the redistribution of dendrons between the upper and lower sub-layers. The fraction α of strongly stretched dendrons increases upon the increase in the grafting density σ to leave more space to weakly stretched dendrons in the first sub-layer (see figure 5 below). The grafting density of starlike macromolecules with f branches cannot exceed the value of

$$\sigma = \sigma^* = \frac{2}{f} \tag{12}$$

corresponding to dense packing of these polymers in the sub-layers (with $\varphi_1 = \varphi_2 = 1$). The fraction of strongly stretched dendrons, corresponding to this dense packing is

$$\alpha = \alpha^* = \frac{f}{2(f-1)} \tag{13}$$

It is shown in Appendix C that eqs 12 and 13 constitute a special case of a more general relationship in planar brushes made of dendrons with arbitrary number generation. Maximal possible density of dendron grafting, σ^*, and the

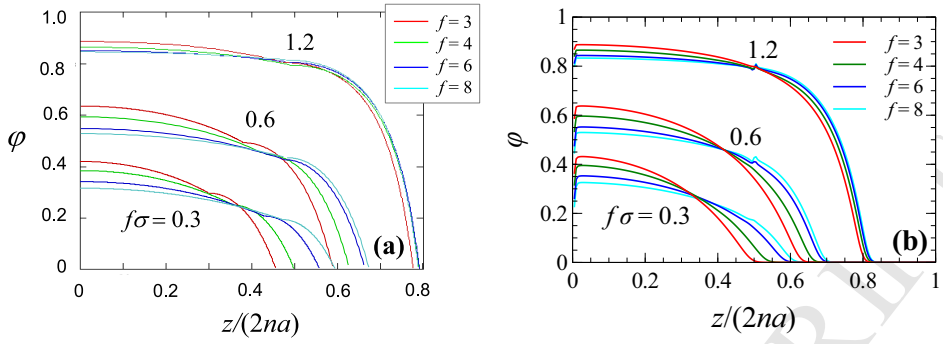

Figure 4: Polymer density profiles (volume fractions) $\varphi(z)$ predicted by the AA model (a) and obtained from the SF-SCF calculations (b) for various values of the product $f\sigma = 0.3$, 0.6 and 1.2.

corresponding fraction α^* of dendrons with strongly stretched stem (root spacer) that pass through the first (inner) sub-layer in a brush with grafting density σ^* are given by

$$\sigma^* = \frac{\mathcal{N}}{N}, \quad \alpha^* = \frac{1 - n/\mathcal{N}}{1 - n/N}, \tag{14}$$

where N is the total number of monomer units in a dendron, $\mathcal{N} = n(g+1)$ is the number of monomer units in the longest path connecting the grafting points and any of the dendron's free end, n is the dendron spacer length, and g is the number of generations in the dendron ($g = 1$ corresponds to a star).

In figure 3 we present thicknesses of sub-layers, $H_1/(an)$ (a), $H_2/(an)$ (b), and the total brush thickness, $H/(2an)$ (c) as a function of re-scaled grafting density, σ/σ^*. In these coordinates the already mentioned difference in behaviors of H_1 and H_2 becomes even more pronounced. H_2 varies smoothly in the whole σ/σ^* range, and the data for H_2 nicely collapses on a single dependence (figure 3b). The plots for H_1 show a strong dependence on the number of arms f and remain separated (figure 3b), which, in turn, inferior the collapse of the total brush thickness, H, on a master curve (figure 3c). As one can see in figure 3c, formation of inner sub-layer with limiting width $H_1 = na$ is virtually completed at smaller values of σ/σ^* in brushes formed by stars with larger number of arms.

In figure 4 we compare the polymer density profiles, φ, predicted by the AA model (figure 4a) and those obtained from the SF-SCF calculations (fig.4b), and discussed previously (see figure 15 in ref [17]). The plots for various values of σ and f are grouped as suggested by the SF-SCF model, that is, at different values of the product $\sigma f = \sigma/2\sigma^*$. A very good correspondence, both qualitative and quantitative, between the polymer density profiles obtained from the AA and SF-SCF models proves that the approximations used in formulation of the approximate analytical (AA) model are reasonable.

In figure 5 we plot the dependence of fraction α of strongly stretched dendrons, predicted by the AA model (figure 5a) as a function of grafting density σ at different values of f and compare them with the results of SF-SCF calculation for the the same values of the parameters (figure 5b which is similar to

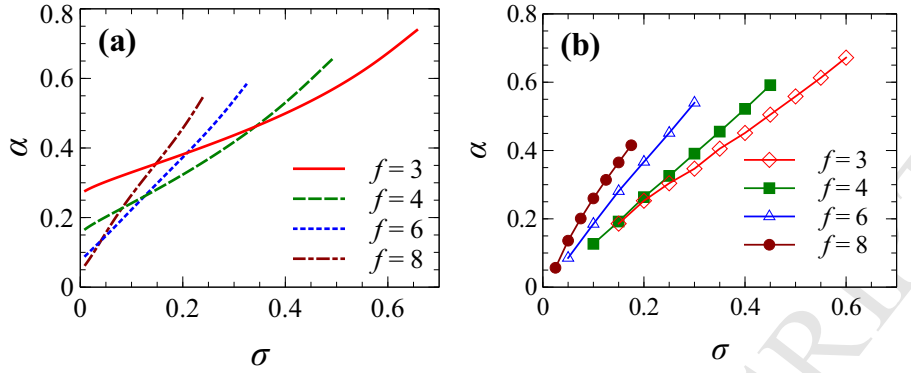

Figure 5: Fraction α of macromolecules in the second sub-layer as a function of grafting density σ predicted by the AA model (a) and obtained from the SF-SCF calculations (b). In panel (b) symbols correspond to data points, lines are drawn to guide the eye.

figure 6 in ref [17]). At large values of $f = 6$ and 8, both models give rather close results, although at small values of f (e.g., $f = 3$), the shape of the analytical dependence $\alpha(\sigma)$ is slightly different from that obtained from the SF-SCF calculation. Good agreement is observed starting from a certain value of σ. At relatively small values of grafting density σ, the dependence of α on f becomes non-monotonous (in figure 5a curves $\alpha(\sigma)$ for different f intersect), while the SF-SCF data (figure 5b) always indicates the monotonous increase in α upon the increase in f at fixed grafting density σ of starlike polymers. We attribute this difference to the increasing inaccuracy of the AA model with the decrease in the grafting density σ and/or in the number of arms f. At dense grafting, however, the values of α calculated from the AA and SF-SCF models become almost identical.

The same data is presented in figure 6 in the re-scaled variables, $x = \sigma f$ and $y = \alpha\sigma(f-1)$, that have been introduced in ref [17]. The predicted by the AA model values of α collapse on the master curve (figure 6a) which is almost similar to the master curve obtained from the SF-SCF calculation (figure 6b which is equivalent to fig. 14 in ref [17]). Note that combination of the parameters, $\alpha\sigma(f-1)$, plotted along y-axis in figure 6 has the meaning of the effective grafting density in the upper brush and is related to α^* and σ^* as $\alpha\sigma(f-1) = \alpha\sigma/(\alpha^*\sigma^*)$.

4 Conclusions

Comparison between the results of SF-SCF numerical calculations and the predictions of the approximate analytical (AA) theory demonstrates a good agreement between the two approaches at large values of the chain grafting density σ and/or at large number of star arms f. The decrease in grafting density σ of star-like polymers leads to inferior of this agreement due to increasing inaccuracy of the AA model. Indeed, the basic assumption of the AA model is the localization of the branching points of strongly stretched dendrons at

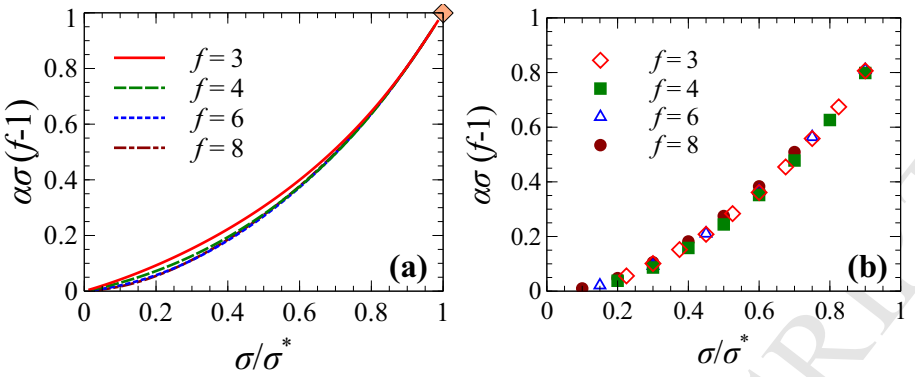

Figure 6: The same data as in figure 5 plotted in re-scaled variables, $y = \alpha\sigma(f-1)$ and $x = \sigma/\sigma^*$. All the lines in panel (a) approach the limiting value of re-scaled variables $y = 1$ and $x = 1$ indicated by a diamond symbol corresponding to $\alpha = \alpha^* = f/[2(f-1)]$ and $\sigma = \sigma^* = 2/f$.

the boundary between the sub-layers, and thereby modeling the upper sub-layer as a monodisperse brush of branches. The decrease in dendron stretching upon a decrease in σ or in the number of branches f places the system in the linear elasticity regime. The two-layer structure of the brush is retained in the linear (Gaussian) elasticity regime for tethered dendrons as well. For starlike polymers with the Gaussian elasticity, the upper sub-layer of thickness $H_2 = H[1-\sqrt{(f-1)/f}]$ contains only polydisperse fragments of the branches, while the lower sub-layer with thickness $H_1 = H\sqrt{(f-1)/f}$contains weakly stretched dendrons and stems with fragments of those branches that pass into the upper sub-layer [17]. However, in contrast to the basic assumption of the AA model about the monodisperse nature of the upper sub-layer (envisioned as the brush of free star arms, each consisting of n monomer units), the upper sub-layer in the brush with the Gaussian elasticity of constituent polymers is polydisperse. Moreover, the branching points of the dendrons in the lower sub-layer are distributed rather uniformly, i.e., without distinct localization at the boundary between two sub-layers (see e.g., fig. 3a in ref. [17] for $f = 3$ and $\sigma = 0.1$).

Therefore, the predictions of the AA model do not cross-over gradually to the results of the analytical model developed in ref. [17] for macromolecules with the Gaussian elasticity (i.e., valid at relatively low grafting densities of starlike dendrons) but are limited to the interval of high values of σ and f. An analytical model which would provide a unified description of the dendron brushes in the two limits of relatively low and high values of σ is still to be developed.

The linear (Gaussian) elasticity regime is rather limited in planar dendron brushes, but it becomes more extended in the cylindrical and spherical geometries. Moreover, the parabolic approximation for molecular potential in curved geometries leads to a progressively smaller error in, e.g., the distribution of the free dendron ends upon chain branching compared to linear chains with the same molecular weight [31]. An increase in the number of generations and/or branching of the dendrons will eventually incur the nonlinear elasticity regime

for the spacers. Therefore, the approximate analytical (AA) model formulated here for starlike polymers can also be extended for the case of curved brushes composed of highly branched dendrons.

Appendix A. Stretching function $E(z)$

To find $E(z)$ one must minimize the free energy functional F for a chain segment of n monomers in the external potential $U_1(z)$ specified by eq 5

$$F = a^{-1} \int_0^{H_1} dz \left\{ [pE - \ln Z(p)] + \frac{U_1(z) + \Lambda_3}{E} \right\} \tag{15}$$

The entropy (in k_B units) of this segment is formulated in square brackets in eq 15, where $p(z)$ is the dimensionless tension force (measured in units of k_BT/a) acting at the distance z from the surface, and $Z(p)$ is the statistical sum of a monomer unit [27]. The second term in eq 15 comprises the contribution due to the potential energy of a segment in the external potential ($dn \cdot U_1 = dz \cdot U_1(z)/E$), and the unknown Lagrangian constant Λ_3, which ensures conservation of the segment length n. For a chain on the bcc lattice, the force p is related to the stretching function E as

$$p = \frac{3}{2} \ln \frac{1+E}{1-E}$$

or, equivalently,

$$\frac{p}{3} = \ln \sqrt{\frac{1+E}{1-E}}$$

Logarithm of the statistical sum of a monomer unit exposed to the force p yields

$$\ln Z(p) = 3 \ln \frac{\exp(p/3) + \exp(-p/3)}{2} = 3 \ln \sqrt{\frac{1}{1-E^2}}$$

and therefore

$$F = a^{-1} \int_0^{H_1} dz \left\{ \frac{3}{2} E \ln \frac{1+E}{1-E} - \frac{3}{2} \ln \frac{1}{1-E^2} + \frac{U_1 + \Lambda_3}{E} \right\}$$

Variation of F with respect to E gives the equation

$$\frac{3}{2} E^2 \ln \frac{1+E}{1-E} = \frac{3}{2} E^2 \ln \frac{(1+E)^2}{1-E^2} = U_1 + \Lambda_3$$

Because of strong stretching of the stem, $E = a^{-1} \cdot dz/dn$ is close to unity. By putting $E \approx 1$, and retaining only the logarithmic divergency, we write

$$\ln \frac{4}{1-E^2} \approx \frac{2}{3}(U_1 + \Lambda) = \ln \cos^2(Kt) + \widetilde{\Lambda}\,,$$

where $K = 2 \arccos \sqrt{(f-1)/f}$ (see eq 2), unknown constant $\widetilde{\Lambda} = \frac{2}{3}(\Lambda_1 + \Lambda_3)$, and $t = z/(2na)$, to give

$$\frac{4}{1-E^2} = \exp(\widetilde{\Lambda}) \cos^2(Kt)$$

By solving this equation, we find

$$E = \sqrt{1 - \frac{4}{\exp\widetilde{(\Lambda)}\cos^2(Kt)}} = \sqrt{1 - \frac{\lambda}{\cos^2(Kt)}}$$

with $\lambda = 4/\exp\widetilde{(\Lambda)}$.

By normalizing the stretching function $E(z)$ as

$$a^{-1}\int_0^{H_1}\frac{dz}{E(z)} = n, \text{ or, equivalently, } a^{-1}\int_0^{h_1}\frac{dt}{E(t)} = 1/2$$

we find

$$\lambda = 1 - \frac{(\sin Kh_1)^2}{(\sin K/2)^2}$$

and specify the stem stretching function as

$$E(t) = \sqrt{1 - \frac{1 - \frac{(\sin Kh_1)^2}{(\sin K/2)^2}}{\cos^2(Kt)}} = \sqrt{1 - \frac{1 - f\sin^2(Kh_1)}{\cos^2(Kt)}} \tag{16}$$

We note that eq 16 reduces to the known expression for stem stretching in dendrons with the Gaussian elasticity if $Kt \ll 1$. Indeed, by expanding the expression for $E(t)$ in eq 16 at $Kt \ll 1$ (that is, by expanding $1/\cos^2(Kt) = 1/[1-\sin^2(Kt)] \approx 1/[1-(Kt)^2] \approx 1+(Kt)^2$, and $\sin^2 K/2 = 1/f$, and $\sin^2 Kh_1 \approx (Kh_1)^2$) we reduce $E(t)$ to

$$E(t) \approx \sqrt{f(Kh_1)^2 - (Kt)^2} = K\sqrt{f{h_1}^2 - t^2}$$

which coincides with the expression in eq 34 in the Appendix in ref [17].

Appendix B. Solution of the set of equations (9), (10), and (11)

The set of three equations: 9, 11, and 10 must be solved numerically. This task can be simplified by the following re-arrangements of these equations.

By extracting $\alpha\sigma/2$ from eq 9 and substituting in eq 11, we find the connection between h_1 and h_2,

$$\frac{\alpha\sigma}{2} = \frac{-3\ln\cos\pi h_2 - 1 + \cos^3\pi h_2}{3\ln\frac{\tan Kh_1 + \tan K/2}{\tan K/2 - \tan Kh_1}} = \frac{-3\ln\cos\pi h_2 - 1 + \cos^3\pi h_2}{3\ln\frac{1+\sqrt{f-1}\tan Kh_1}{1-\sqrt{f-1}\tan Kh_1}}$$

$$(f-1)\left(\frac{-3\ln\cos\pi h_2 - 1 + \cos^3\pi h_2}{3\ln\frac{1+\sqrt{f-1}\tan Kh_1}{1-\sqrt{f-1}\tan Kh_1}}\right) = h_2 - \frac{\cos^3(\pi h_2)}{2\pi}\left[\frac{\sin(\pi h_2)}{\cos^2(\pi h_2)} + \ln\sqrt{\frac{1+\sin(\pi h_2)}{1-\sin(\pi h_2)}}\right]$$

to give

$$\ln\frac{1+q\tan Kh_1}{1-\sqrt{q}\tan Kh_1} = \frac{f-1}{3}\frac{[-3\ln\cos\pi h_2 - 1 + \cos^3\pi h_2]}{h_2 - \frac{\cos^3(\pi h_2)}{2\pi}\left[\frac{\sin(\pi h_2)}{\cos^2(\pi h_2)} + \ln\sqrt{\frac{1+\sin(\pi h_2)}{1-\sin(\pi h_2)}}\right]}$$

$$\frac{1+\sqrt{q}\tan Kh_1}{1-\sqrt{q}\tan Kh_1}=\exp\left\{\frac{f-1}{3}\frac{[-3\ln\cos\pi h_2-1+\cos^3\pi h_2]}{h_2-\frac{\cos^3(\pi h_2)}{2\pi}\left[\frac{\sin(\pi h_2)}{\cos^2(\pi h_2)}+\ln\sqrt{\frac{1+\sin(\pi h_2)}{1-\sin(\pi h_2)}}\right]}\right\}$$

$$\tan Kh_1=\frac{1}{\sqrt{f-1}}\frac{-1+\exp\left\{\frac{f-1}{3}\frac{[-3\ln\cos\pi h_2-1+\cos^3\pi h_2]}{h_2-\frac{\cos^3(\pi h_2)}{2\pi}\left[\frac{\sin(\pi h_2)}{\cos^2(\pi h_2)}+\ln\sqrt{\frac{1+\sin(\pi h_2)}{1-\sin(\pi h_2)}}\right]}\right\}}{1+\exp\left\{\frac{f-1}{3}\frac{[-3\ln\cos\pi h_2-1+\cos^3\pi h_2]}{h_2-\frac{\cos^3(\pi h_2)}{2\pi}\left[\frac{\sin(\pi h_2)}{\cos^2(\pi h_2)}+\ln\sqrt{\frac{1+\sin(\pi h_2)}{1-\sin(\pi h_2)}}\right]}\right\}}$$

and finally we find $h_1=h_1(h_2)$ as

$$h_1(h_2)=\frac{1}{K}a\tan\left[\frac{1}{\sqrt{f-1}}\frac{-1+\exp\left\{\frac{f-1}{3}\frac{[-3\ln\cos\pi h_2-1+\cos^3\pi h_2]}{h_2-\frac{\cos^3(\pi h_2)}{2\pi}\left[\frac{\sin(\pi h_2)}{\cos^2(\pi h_2)}+\ln\sqrt{\frac{1+\sin(\pi h_2)}{1-\sin(\pi h_2)}}\right]}\right\}}{1+\exp\left\{\frac{f-1}{3}\frac{[-3\ln\cos\pi h_2-1+\cos^3\pi h_2]}{h_2-\frac{\cos^3(\pi h_2)}{2\pi}\left[\frac{\sin(\pi h_2)}{\cos^2(\pi h_2)}+\ln\sqrt{\frac{1+\sin(\pi h_2)}{1-\sin(\pi h_2)}}\right]}\right\}}\right] \tag{17}$$

By summing eqs 11 and 10, we relate h_2 to grafting density σ,

$$h_2-\frac{\cos^3(\pi h_2)}{2\pi}\left[\frac{\sin(\pi h_2)}{\cos^2(\pi h_2)}+\ln\sqrt{\frac{1+\sin(\pi h_2)}{1-\sin(\pi h_2)}}\right]+$$

$$+h_1-\frac{\cos^3(\pi h_2)\cos^3(Kh_1)}{2K}\left[\frac{\sin(Kh_1)}{\cos^2(Kh_1)}+\ln\sqrt{\frac{1+\sin(Kh_1)}{1-\sin(Kh_1)}}\right]=\frac{\sigma f}{2} \tag{18}$$

where $h_1(h_2)$ is specified by eq 17.

We solve the above equation 18 numerically to find the dependence of h_2 on σ. Then by using eq 11, we specify the fraction α of strongly stretched starlike dendrons. This scheme was utilized to compare the predictions of AA-model with the results of SF -SCF modeling [17].

Appendix C. Maximum grafting density in dendron brush

Consider a planar brush made of regularly branched treelike macromolecules, or dendrons, attached to the surface by their root segments (focal points) at the grafting density σ. Dendrons in the brush are assumed to be identical, a dendron is characterized by the generation g and a functionality $q \geq 2$ of each branching point. As it was demonstrated earlier [15, 16, 18, 24], starting from a certain grafting density, grafted dendrons partition into two or more populations differing in the degree of stretching. The number of dendron populations simultaneously coexisting in the brush grows with increasing grafting density up to the maximal value of $g+1$. The brush, therefore, acquires a stratified structure. The first layer, adjacent to the grafting surface, contains the fraction $(1-\alpha)$ of weakly stretched dendrons while the rest of dendrons (fraction α)

"contribute" only their extended root spacers to this layer. The second layer is a brush made of dendrons of generation $(g-1)$ grafted at the effective density $\sigma_{eff} = \sigma\alpha q$. The maximal grafting density corresponds to the condition of dense (solvent-free) packing of dendrons, and the brush height at this grafting density is equal to the contour length of the longest path connecting the grafting point and a free end of a dendron: $H = H_{max} = \mathcal{N}a = (g+1)na$. Since the height of a solvent-free (dry) brush is expressed via the grafting density and the overall number of monomer units in the dendron as N as $H = Na\sigma$, then

$$\sigma^* = \frac{\mathcal{N}}{N}. \tag{19}$$

The width of the first sub-layer at the maximal grafting density σ^* is equal to na. On the other hand it can be expressed as $H_1 = [N(1-\alpha^*) + n\alpha^*]a\sigma$. Hence, the fraction of dendrons that pass through the first sub-layer at maximal grafting density σ^* equals

$$\alpha^* = \frac{1 - n/\mathcal{N}}{1 - n/N}. \tag{20}$$

Acknowledgments

This research was supported by a Marie Curie International Research Staff Exchange Scheme Fellowship (PIRSES-GA-2013-612562 - POLION) within the 7th European Community Framework Programme and partially supported by the Russian Foundation for Basic Research (Grant 14-03-00372a), by the Department of Chemistry and Material Science of the Russian Academy of Sciences and by Government of Russian Federation, Grant 074-U01.

References

[1] Alexander, S. *J. Phys. (France)*, **1977**, *38*, 983.

[2] de Gennes, P.-G. *Macromolecules*, **1980**, *13*, 1069.

[3] Napper, D.H. *Polymeric Stabilization of Colloidal Dispersions*, Academic Press, London, 1985.

[4] Zhao, B.; Brittain, W.J. *Progr. Polym. Sci.* **2000**, *25*, 677.

[5] Cohen Stuart, M. A.; Huck, W. T. S.; Genzer, J.; Müller, M.; Ober, C.; Stamm, M.; Sukhorukov, G. B.; Szleifer, I.; Tsukruk, V.V.; Urban, M.; Winnik, F.; Zauscher, S.; Luzinov, I.; Minko, S. *Nat. Mater.* **2010**, *9*, 101.

[6] Jain, P.; Baker, G.L.; Bruening, M.L. *Annu. Rev. Anal. Chem.* **2009**, *2*, 387.

[7] Birshtein, T.M.; Amoskov, V.M. *Polym. Sci.* **2000**, C42, *2*, 172.

[8] *Polymer Brushes*, Ed. V. Mittal, CRC Press, 2012

[9] Fleer, G.J.; Cohen Stuart, M.A.; Scheutjens, J.M.H.M.; Cosgrove, T.; Vincent, B. *Polymers at Interfaces*, Chapman & Hall, London, 1993.

[10] Gillich, T.; Benetti, E.M.; Rakhmatullina, E.; Konradi, R.; Li, W.; Zhang, A.; Schlüter, A.D.; Textor, M. *J. Am. Chem. Soc.* **2011**, *133*, 10940.

[11] Schüll, C.; Frey, H. *Polymer* **2013**, *54*, 5443.

[12] Pickett, G. T. *Macromolecules* **2001**, *34*, 8784.

[13] Götze, I.O.; Likos, C.N. *Macromolecules* **2003**, *36*, 8189.

[14] Kröger, M.; Peleg, O.; Halperin, A. *Macromolecules* **2010**, *43*, 6213.

[15] Polotsky, A.A.; Gillich, T.; Borisov, O.V.; Leermakers, F.A.M.; Textor, M.; Birshtein, T.M. *Macromolecules* **2010**, *43* 9555.

[16] Merlitz, H.; Wu, C.-X.; Sommer, J.-U. *Macromolecules* **2011**, *44*, 7043.

[17] Polotsky, A.A.; Leermakers, F.A.M.; Zhulina, E.B.; Birshtein, T.M. *Macromolecules* **2012**, *45* 7260.

[18] Gergidis, L.N.; Kalogirou, A.; Vlahos, C. *Langmuir* **2012**, *28*, 17176.

[19] Merlitz, H.; Cui, W.; Wu, C.-X.; Sommer, J.-U. *Macromolecules* **2013**, *46*, 1248.

[20] Guo, Y.; van Beek, J.D.; Zhang, B.; Colussi, M.; Walde, P.; Zhang, A.; Kröger, M.; Halperin, A.; Schlüter, A.D. *J. Am. Chem. Soc.* **2009**, *131*, 11841.

[21] Borisov, O.V.; Zhulina, E.B.; Birshtein, T.M. *ACS Macro Lett.* **2012** *1*, 1166.

[22] Rud, O.V., Polotsky, A.A.; Gillich, T.; Borisov, O.V.; Leermakers, F.A.M.; Textor, M.; Birshtein, T.M. *Macromolecules* **2013**, *46*, 4651.

[23] Gergidis, L.N., Kalogirou, A.; Charalambopoulos, A.; Vlahos, C. *J. Chem. Phys.* **2013**, *139*, 044913.

[24] Borisov, O.V.; Polotsky, A.A.; Rud, O.V., Zhulina E.B.; Leermakers, F.A.M.; Birshtein, T.M. *Soft Matter* **2014**, *10*, 2093.

[25] Boublik, T. *J. Chem. Phys.* **1970**, *53*, 471. Mansoori, G. A.; Carnahan, N. F.; Starling, K. E.; Leland, T. W. *ibid.* **1971**, *54*, 1523.

[26] Amoskov, V.M.; Pryamitsyn, V.A. *J. Chem. Soc. Faraday Trans.* **1994**, *90*, 889.

[27] Amoskov, V.M.; Pryamitsyn, V.A. *Macromol. Theory Simul.* **2003**, *12*, 223.

[28] Amoskov, V.M. ; Pryamitsyn, V.A. *Polym. Sci. (Russia) Ser. A* **1995**, *37*, 731.

[29] Semenov, A.N. *Sov. Phys. JETP* **1985**, *61*,733.

[30] Skvortsov,A.M.; Pavlushkov, I.V.; Gorbunov, A.A.; Zhulina, E.B.; Borisov, O.V.; Pryamitsyn, V.A. *Polym. Sci. (USSR)* **1988**, *30*, 1706

[31] Zook, T.C.; Pickett, G.T. *Phys. Rev. Lett.* **2003**, *90* (1), 015502.

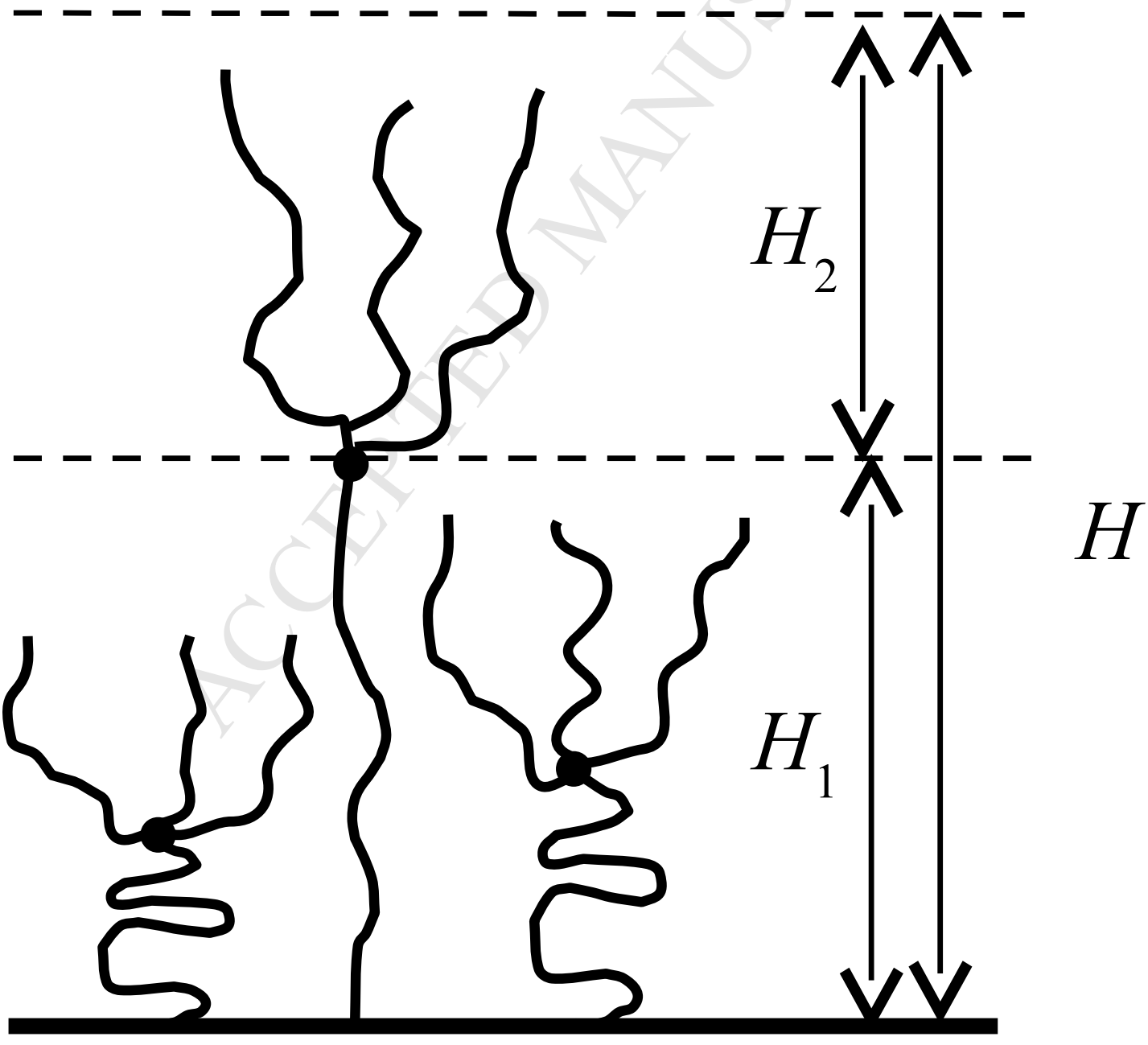

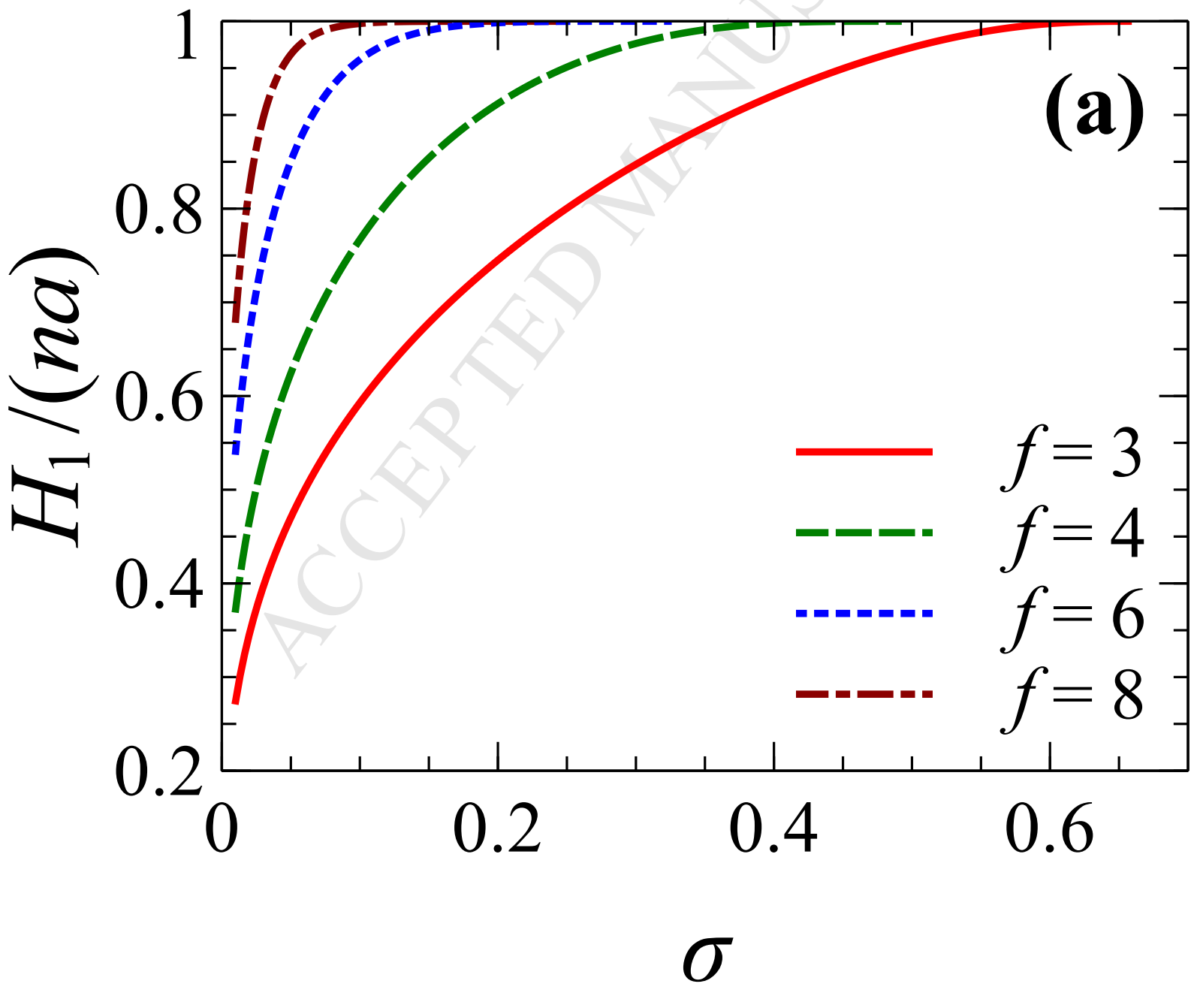

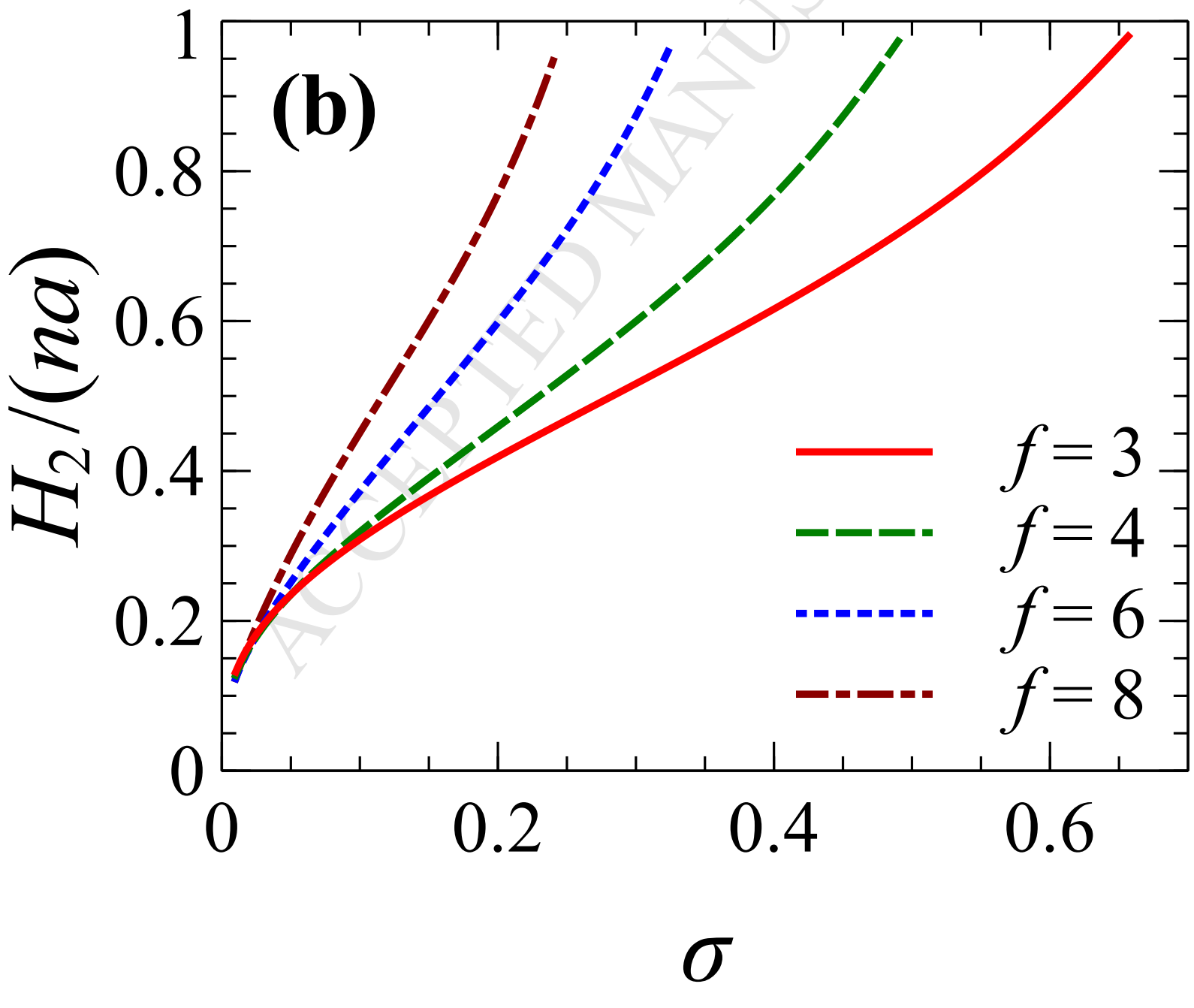

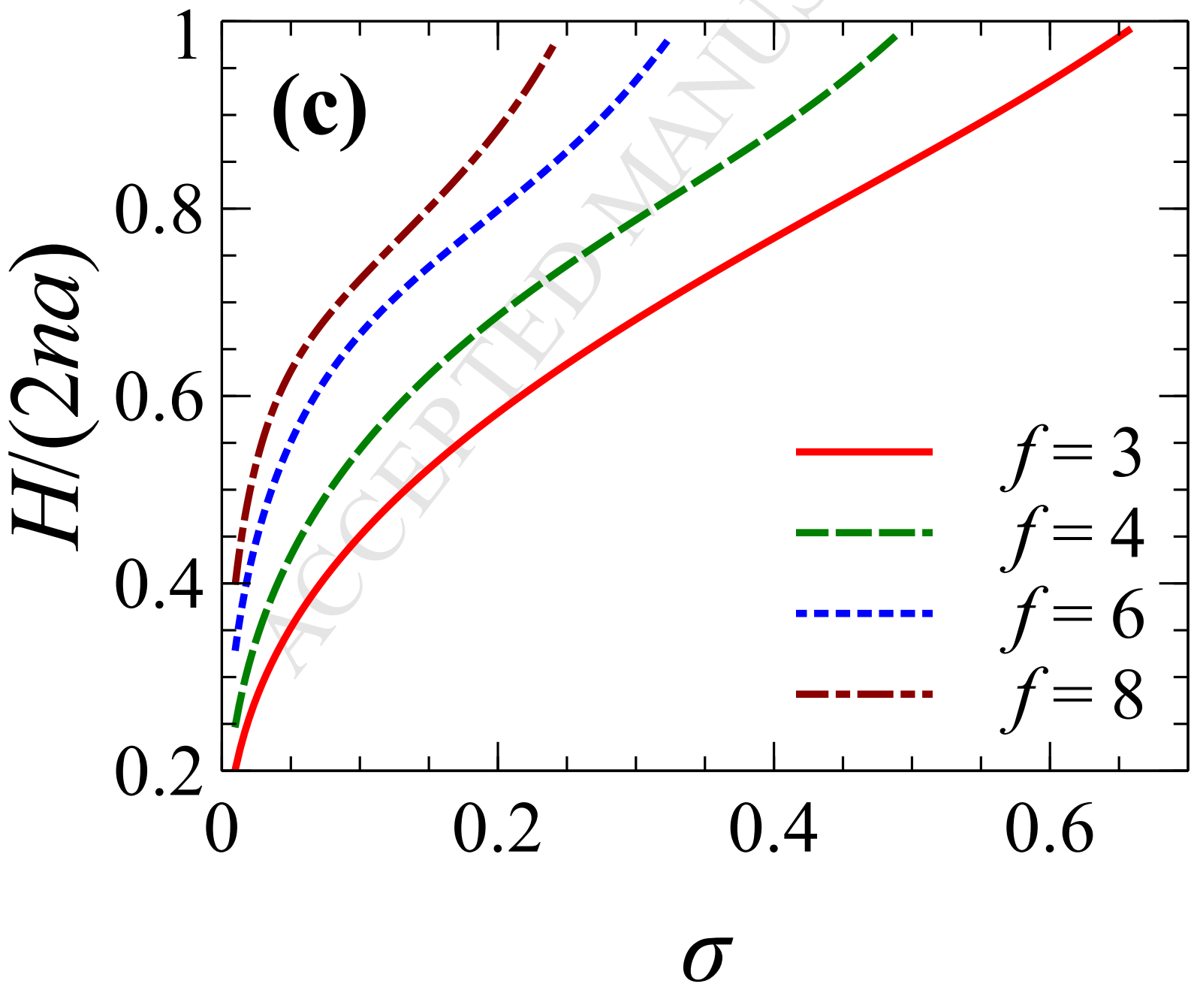

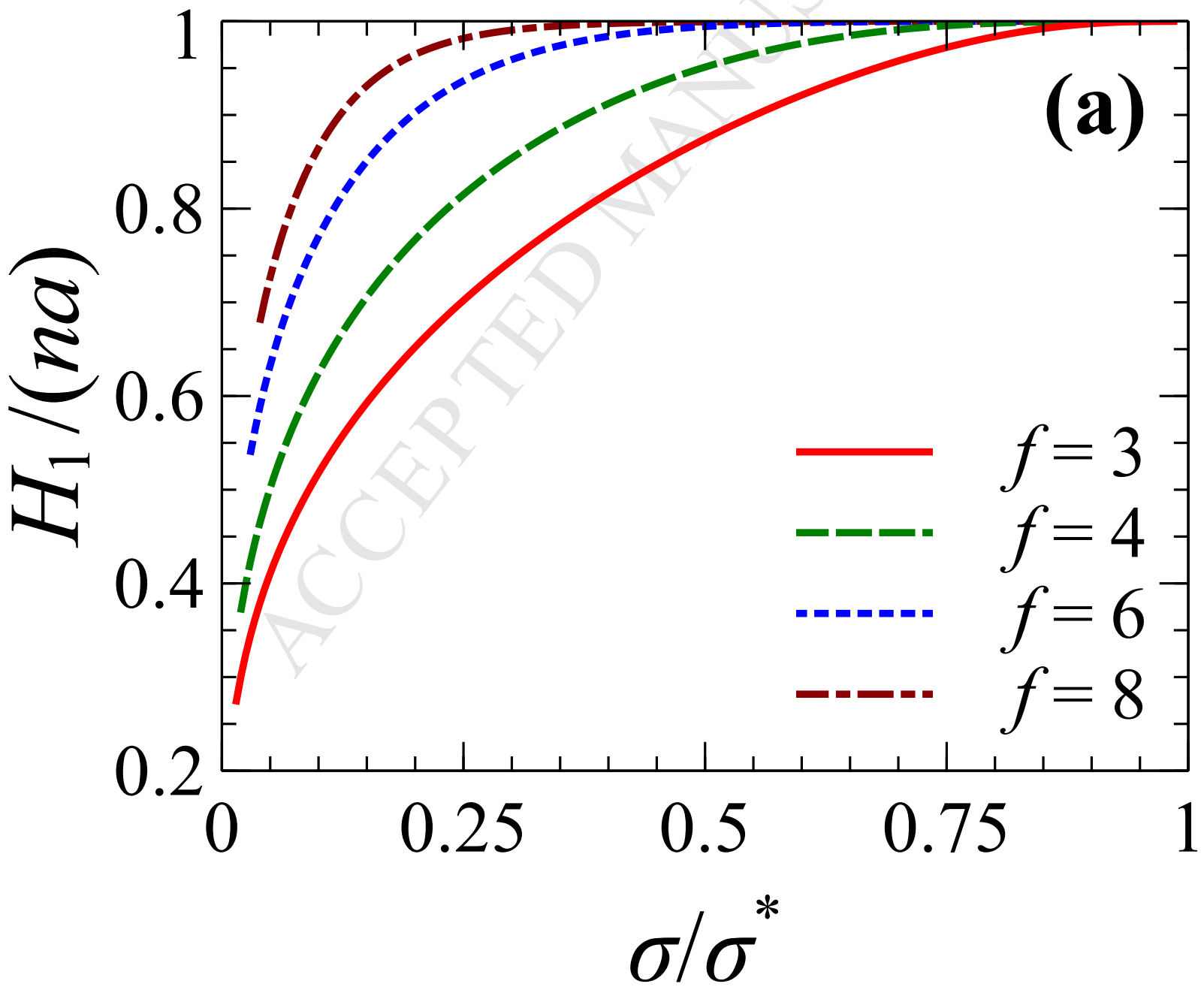

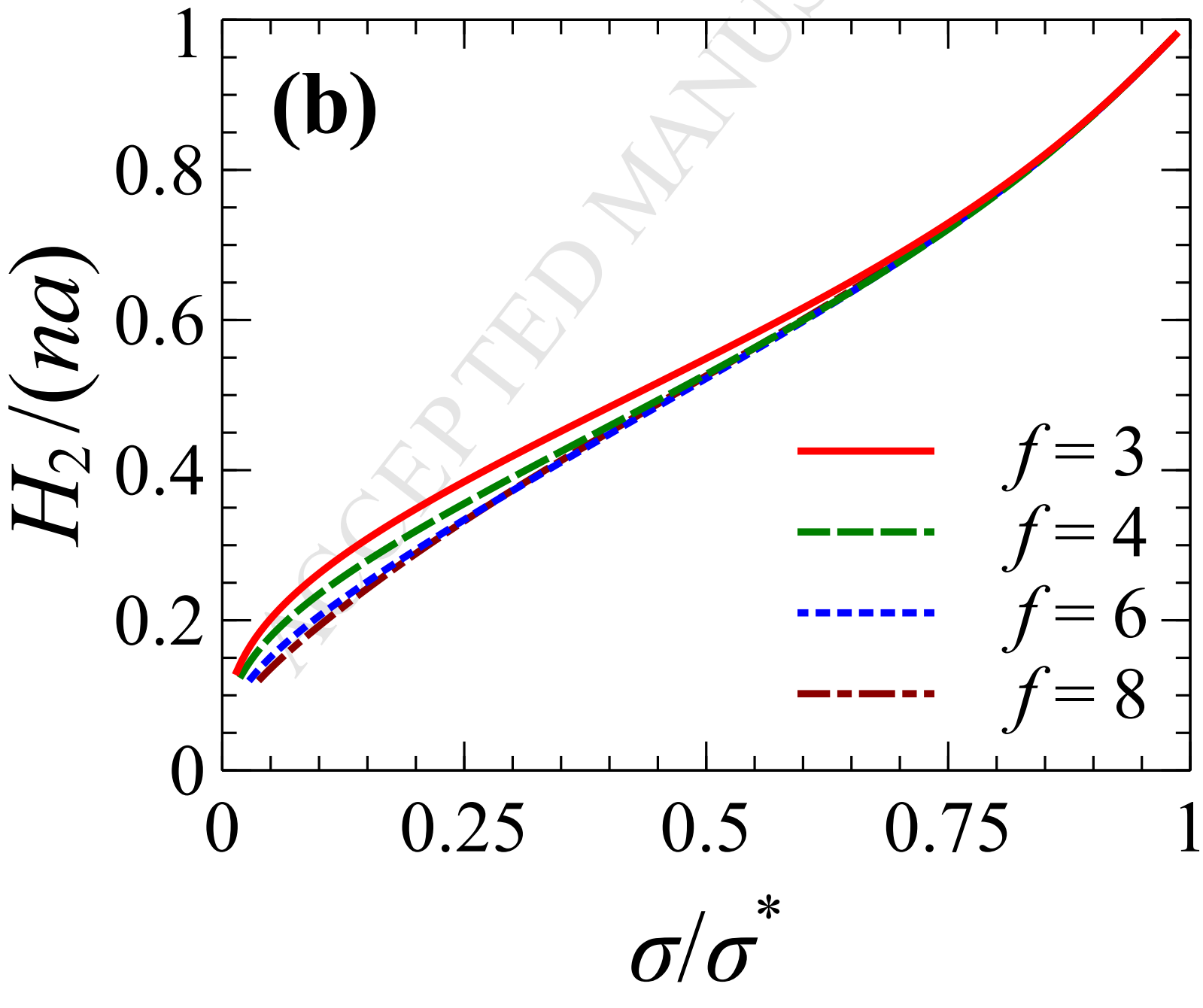

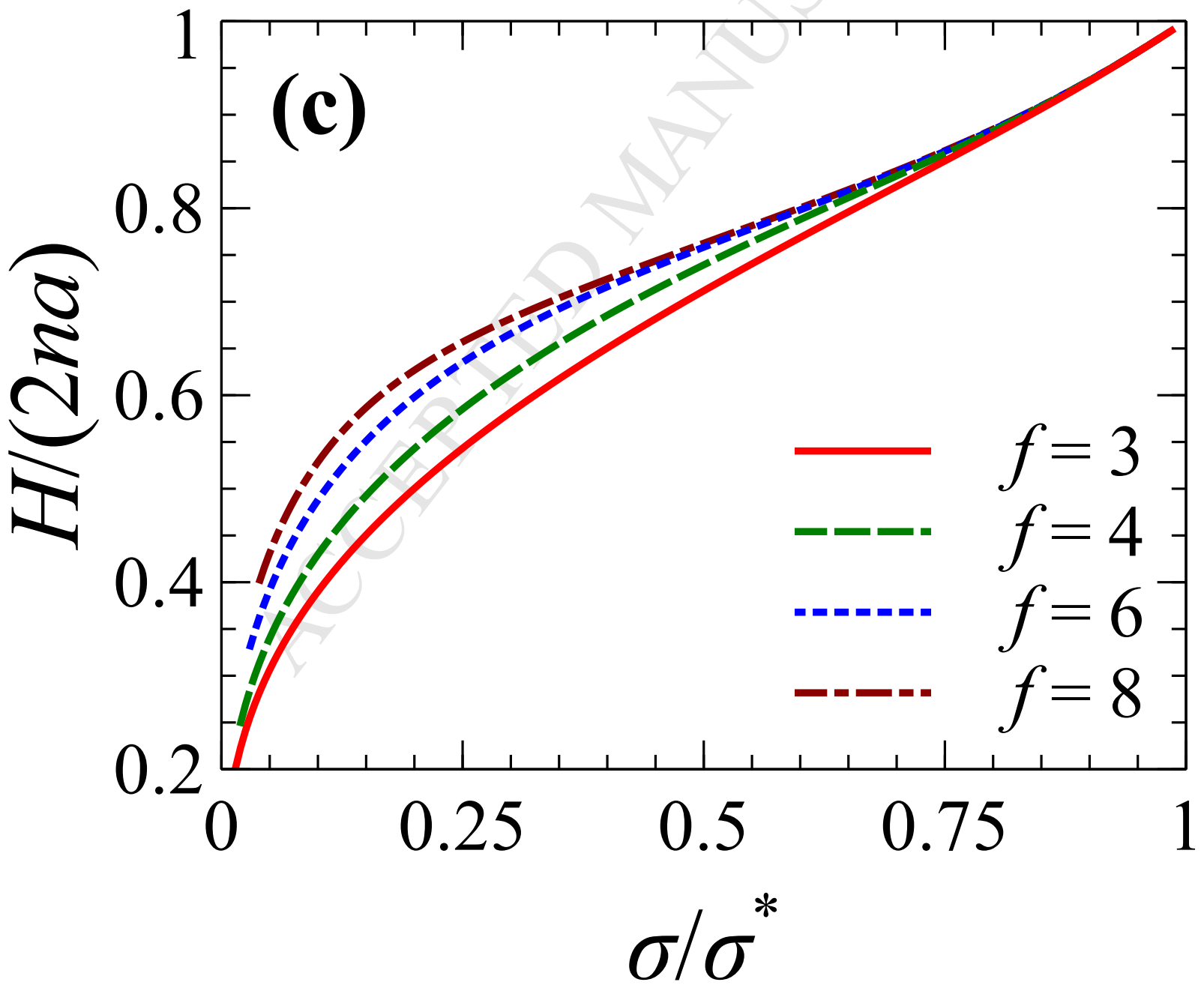

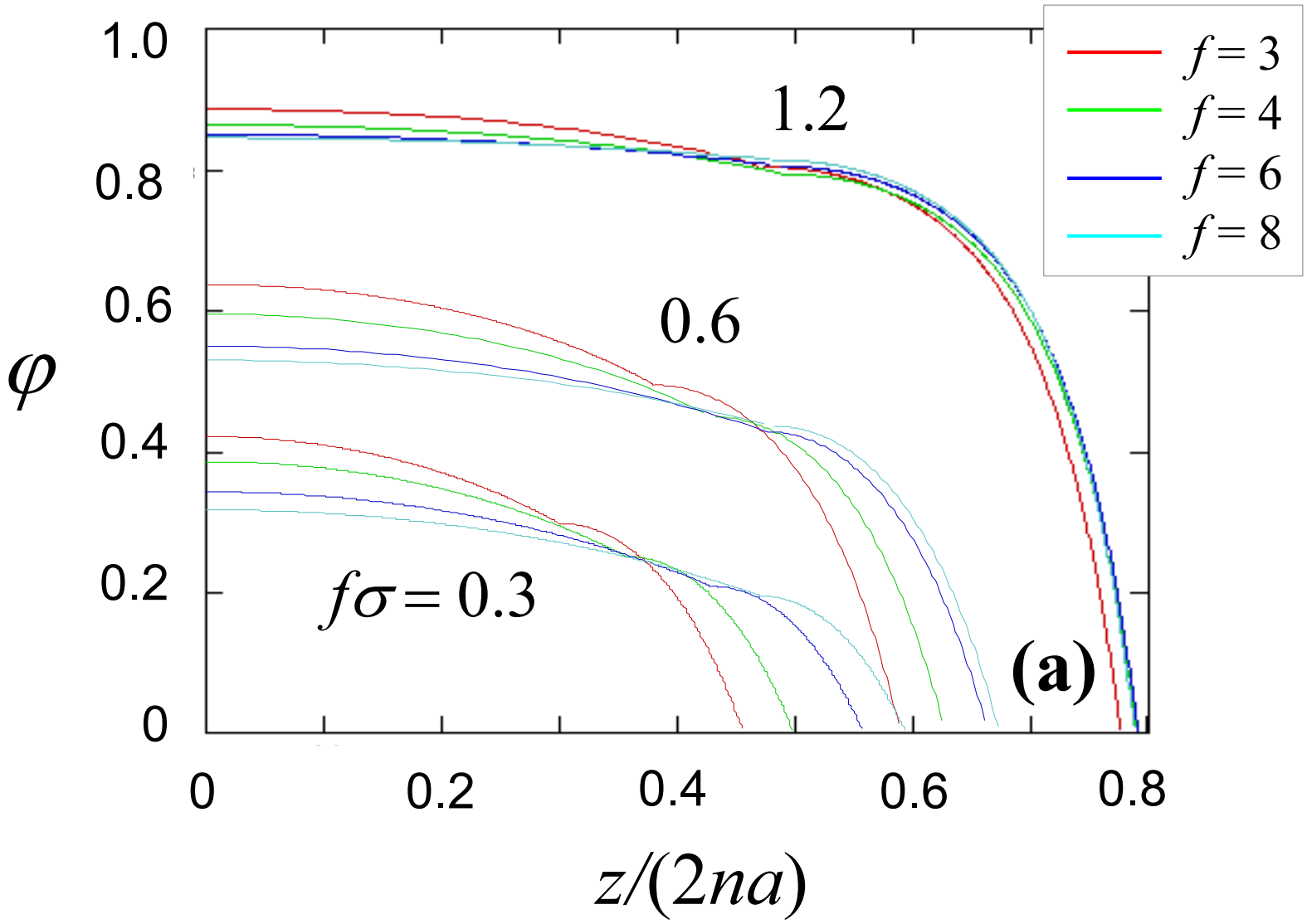
1.0
0.8
0.6
0.4
0.2
0
0
0.2
0.4
0.6
0.8
φ
z/(2na)
1.2
0.6
fσ = 0.3
(a)
f = 3
f = 4
f = 6
f = 8

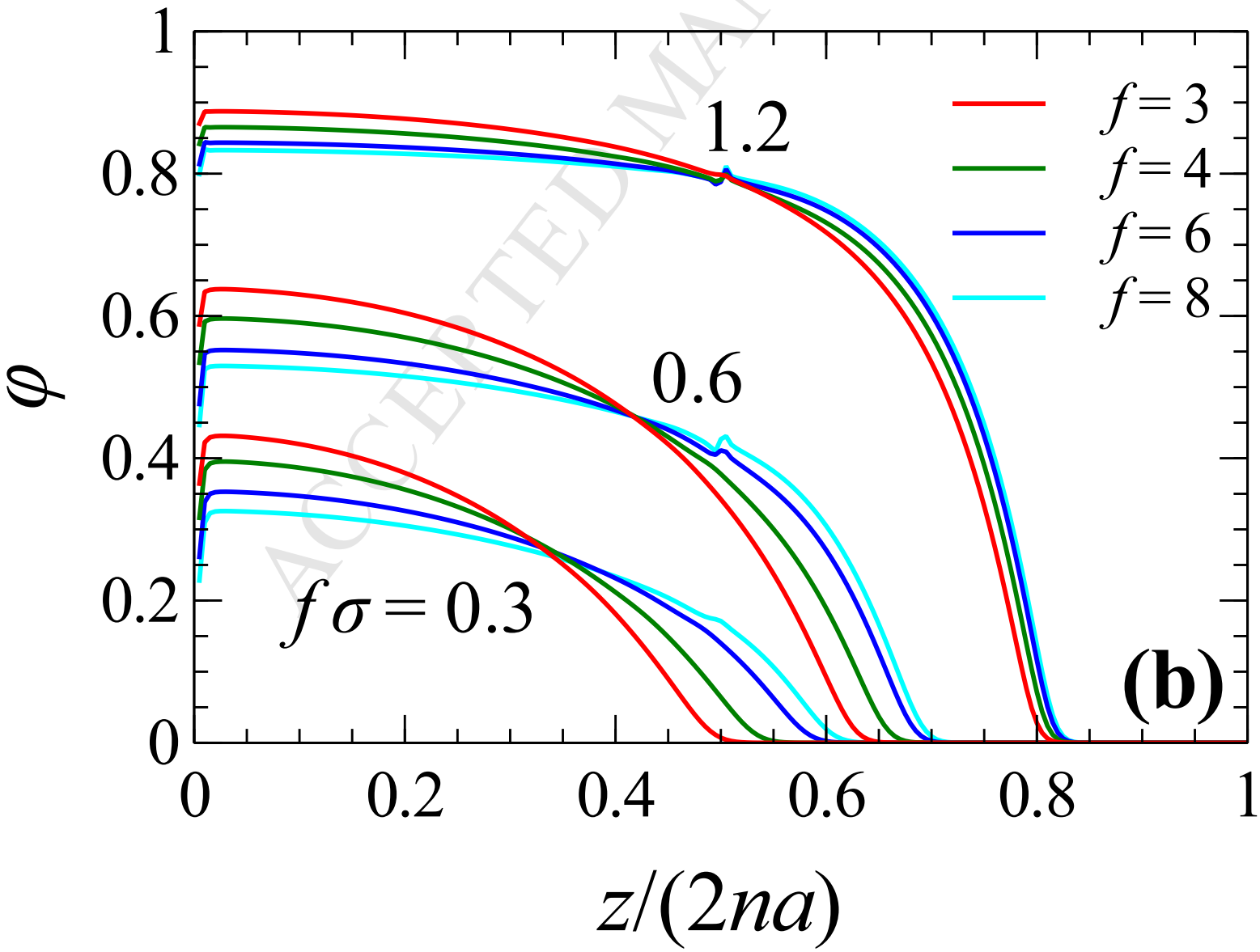

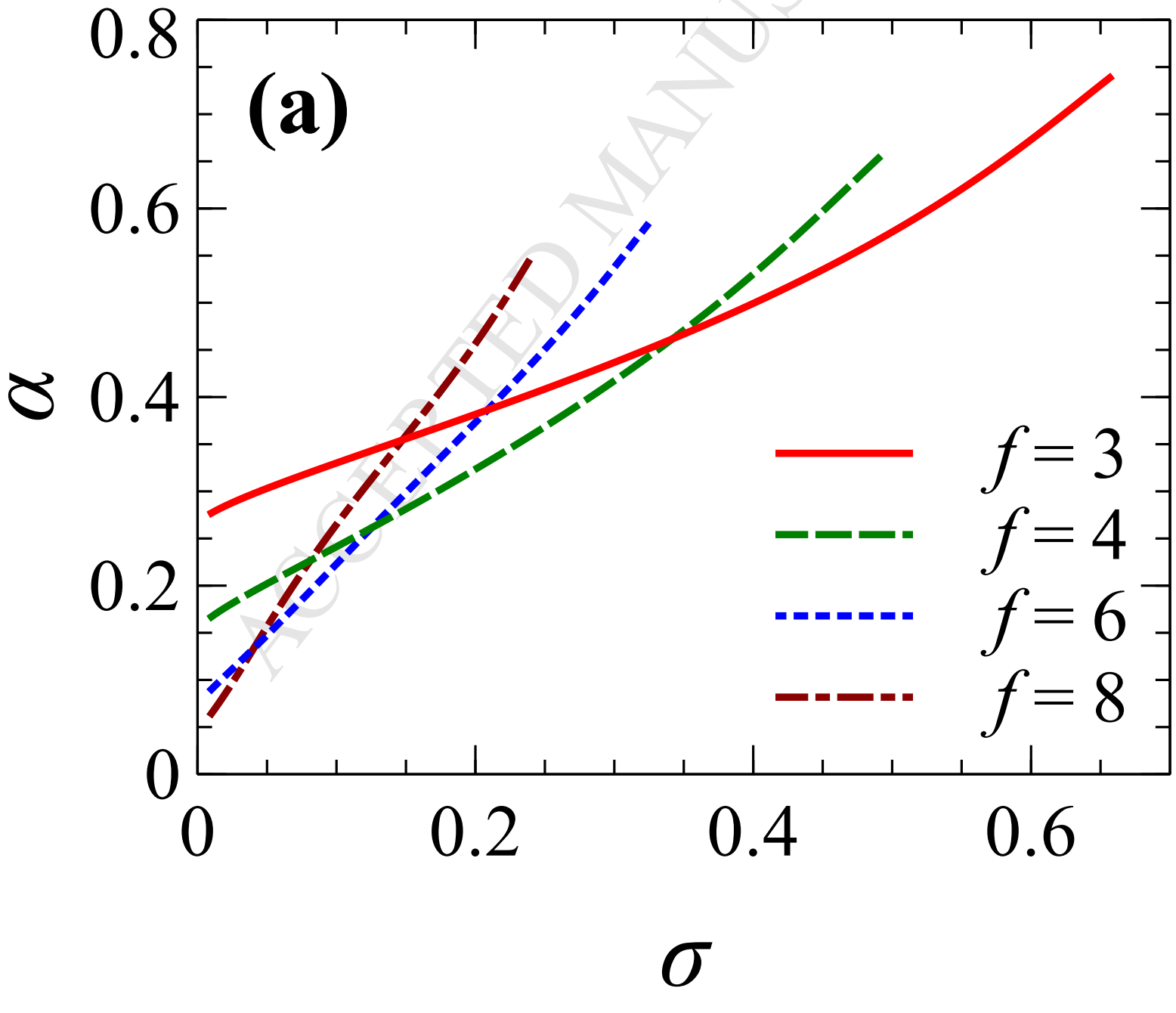

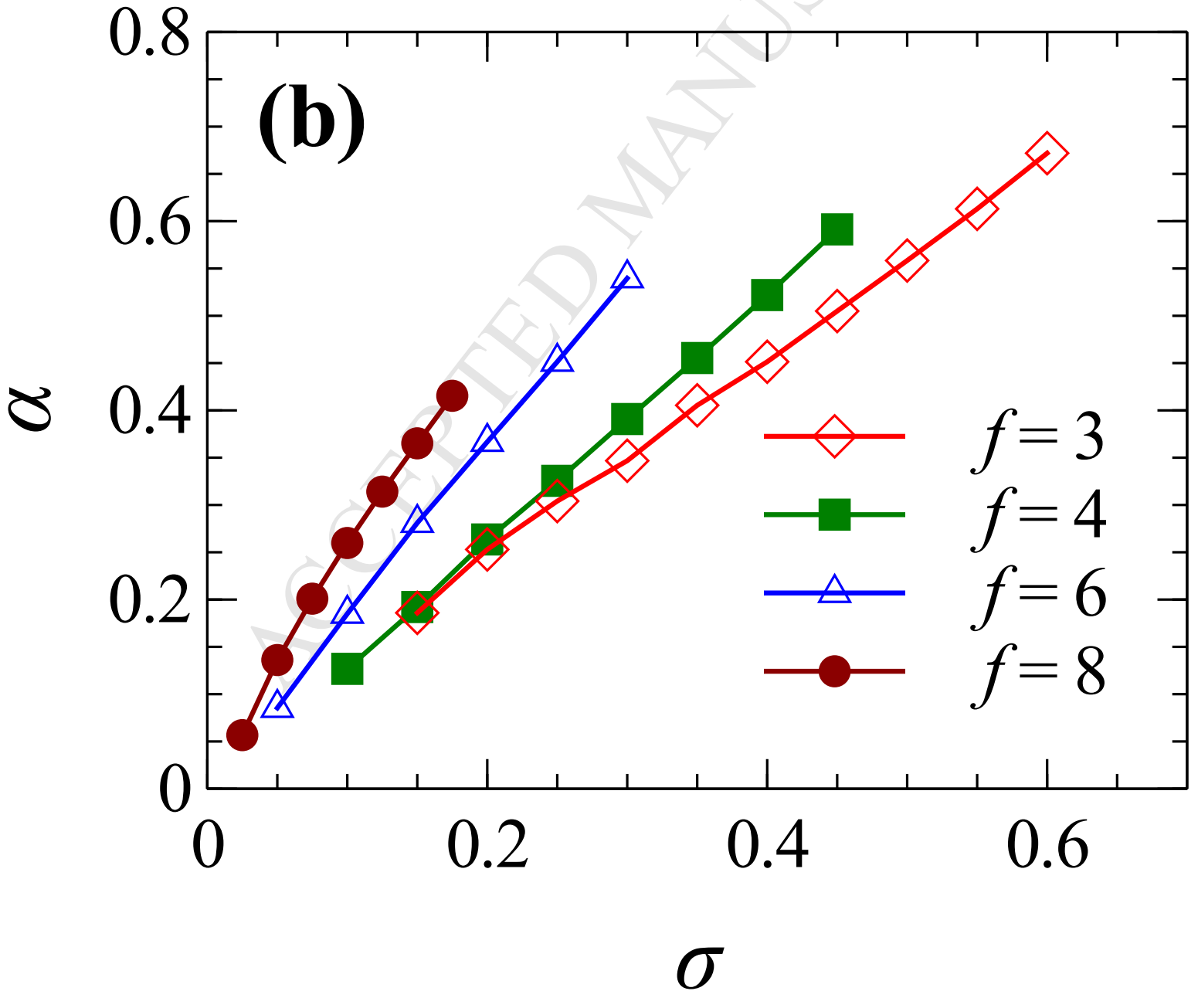

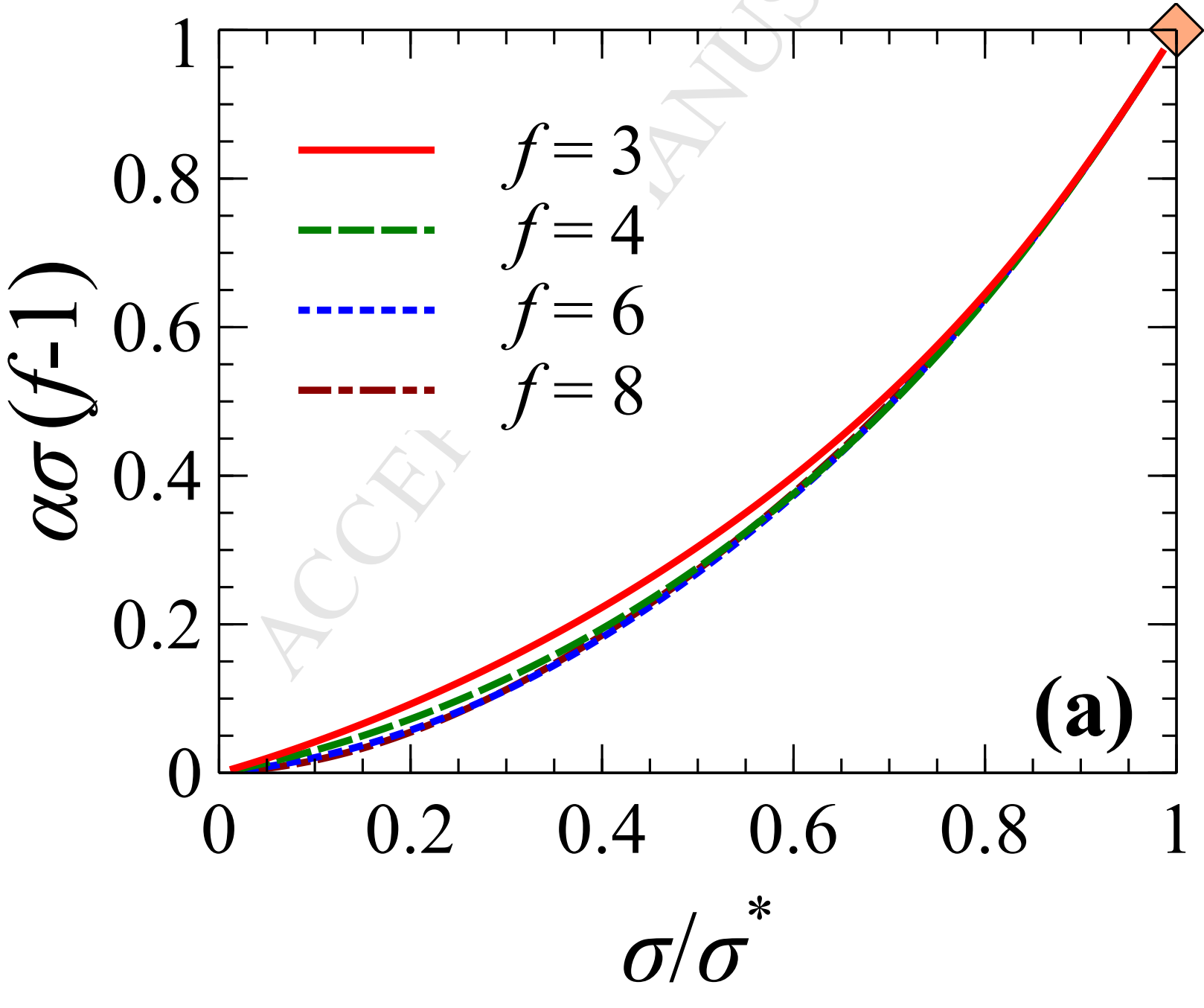

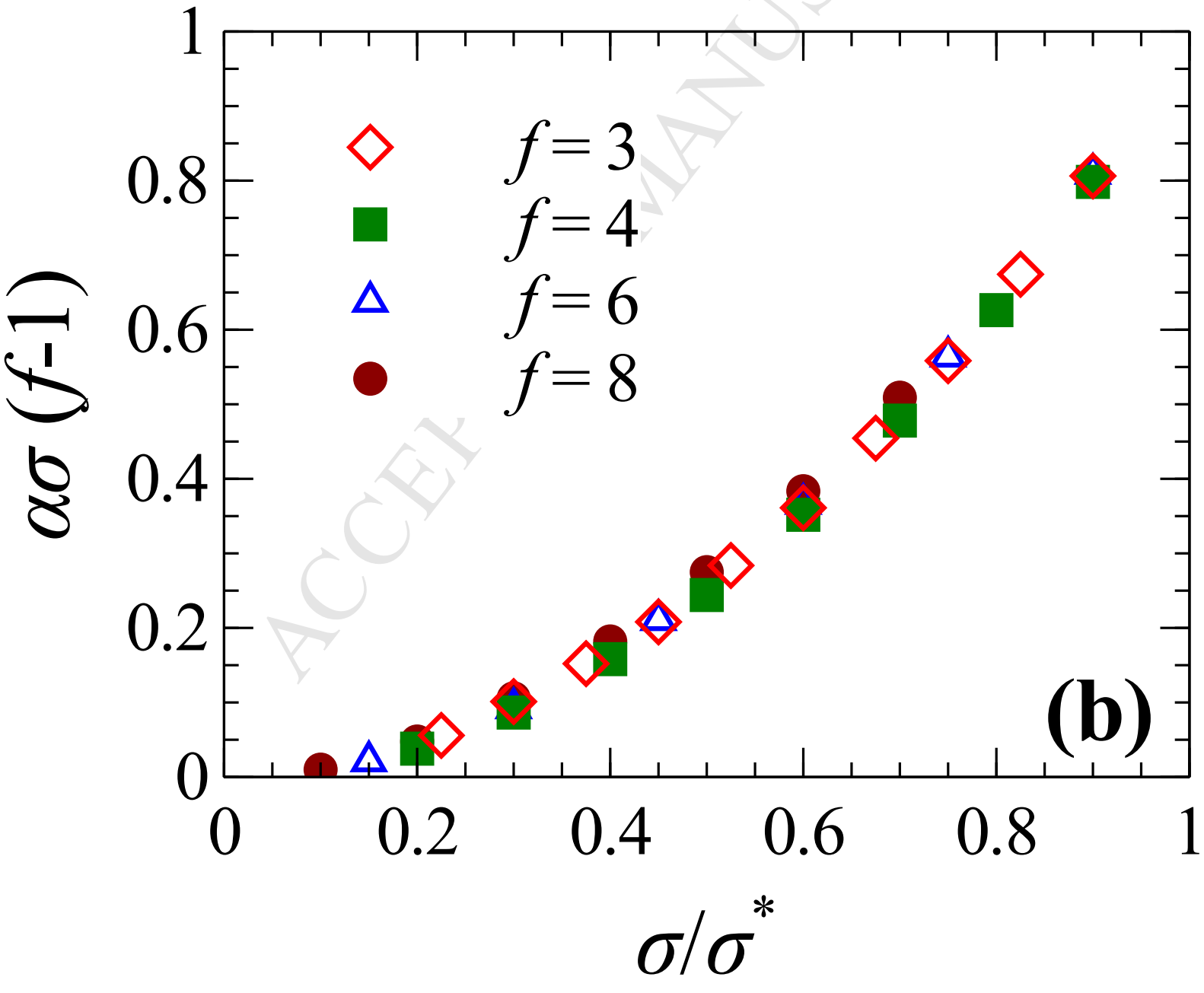

- We develop approximate analytical theory of a planar brush made of starlike polymers.
- The theory takes into account the two-layer structure of the brush.
- We calculate polymer density profiles, brush thickness and fraction of strongly stretched stars.
- We compare results of the analytical theory and numerical self-consistent field modeling.
- We observe a good agreement between analytical and numerical approaches.